

FREQUENCY STANDARDS

https://doi.org/10.1070/QEL16943

Acousto-optic modulators for a controlled frequency shift of light beams in optical and microwave cold-atom frequency standards

V.M. Epikhin, V.N. Baryshev, S.N. Slyusarev, A.V. Aprelev, I.Yu. Blinov

Abstract. **A series of specialised acousto-optic modulators/frequency shifters based on paratellurite (TeO_2) single crystals is developed for systems of laser cooling and frequency stabilisation of laser sources in optical and microwave frequency standards based on cold strontium, rubidium and caesium atoms. The methods of calculation and optimisation of the main parameters of acousto-optic modulators are considered; their basic technical characteristics are experimentally investigated in the spectral range of optical radiation 460–900 nm and in the frequency shift range of 5–400 MHz. The modulators have a high diffraction efficiency, low power consumption and the ability to work with linearly and randomly polarised optical radiation.**

Keywords: *acousto-optic diffraction, frequency shift, frequency shifter, modulator, laser cooling, frequency stabilisation, frequency standards.*

1. Introduction

The relevance of developing highly efficient tunable frequency shifters is due, first, to their active use in laser cooling systems, which are a flexible and effective tool for the formation of atomic ensembles in the quantum frequency standards (QFS's) of the optical and microwave range [1]. After passing through the frequency shifter, the laser beam retains its inherent properties (coherence, directivity, spectral brightness, angular and spatial intensity distributions), and in addition there is the possibility of controlled frequency tuning in the range of hundreds of megahertz, which ultimately allows atomic beams to be cooled down to a temperature of several microkelvins [2–4].

The frequency shift of the radiation beam can be obtained using various methods of its modulation. For example, in the case of amplitude modulation, the spectrum simultaneously contains symmetrical components with positive and negative shifts of the initial frequency by the modulation frequency, and the intensity of each component does not exceed 25% of the intensity of the unmodulated radiation beam. When using one component, this method is not efficient.

In the Bragg regime of acousto-optic (AO) diffraction, in addition to the undiffracted beam, only the first diffraction order is formed, and its intensity can reach the intensity of the incident radiation beam [5, 6]. The frequency shift of the diffracted light wave is a consequence of the laws of energy and momentum conservation for photons of the incident and diffracted light beams and phonons of the ultrasonic wave (USW), which are formulated below:
when a phonon is absorbed

$$\omega_0 + \Omega = \omega_\mathrm{d},$$

$$\boldsymbol{k}_0 + \boldsymbol{q} = \boldsymbol{k}_\mathrm{d},$$

when a phonon is created

$$\omega_0 = \omega_\mathrm{d} + \Omega, \qquad \omega_\mathrm{d} = \omega_0 - \Omega,$$

or

$$\boldsymbol{k}_0 = \boldsymbol{k}_\mathrm{d} + \boldsymbol{q}, \qquad \boldsymbol{k}_\mathrm{d} = \boldsymbol{k}_0 - \boldsymbol{q},$$

where ω_0 and ω_d are the photon frequencies of the incident and diffracted light beams; Ω and $\boldsymbol{q}$ are the frequency and wave vector of the phonon of the ultrasound wave; and $\boldsymbol{k}_0$ and $\boldsymbol{k}_\mathrm{d}$ are the wave vectors of the photons of the incident and diffracted light beams.

In anisotropic diffraction the tips of the wave vectors of the incident ($\boldsymbol{k}_0$) and diffracted ($\boldsymbol{k}_\mathrm{d}$) light waves lie on different second-order wave surfaces, a sphere and an ellipsoid, while in isotropic diffraction they are on a single surface, a sphere. Therefore, in the first case, the polarisation directions of the incident and diffracted beams are mutually orthogonal, and in the second case, they are parallel.

Figure 1 shows the vector diagrams for AO diffraction in the Bragg regime with phonon absorption (creation), where the frequency of the diffracted light beam increases (decreases) by the ultrasound frequency Ω. Thus, using one AO device, one can obtain both positive and negative frequency shifts. These advantages distinguish AO diffraction from other methods of obtaining a frequency shift.

Recently, AO frequency shifters have found a new application in systems for controlling the frequency and intensity of laser sources in QFS's. In this case, the AO frequency shifter operates in the pure Raman–Nath regime, and the error signal when the radiation frequency of the diode laser is automatically adjusted to the frequency of the optical resonance is formed simultaneously by ± 1 and zero diffraction orders [7]. As studies have shown, this method has several advantages both in frequency modulation spectroscopy [8, 9] and in modulation transfer spectroscopy [10].

The question arises about the possible effect of USWs on the light wave temporal stability. If the absolute values of the frequency uncertainty for the light and sound waves are

V.M. Epikhin, V.N. Baryshev, S.N. Slyusarev, A.V. Aprelev, I.Yu. Blinov All-Russian Scientific Research Institute of Physical-Technical and Radiotechnical Measurements (VNIIFTRI), 141570 Mendeleevo, Moscow region, Russia; e-mail: epikvm@mail.ru

Received 26 December 2018; revision received 22 March 2019
Kvantovaya Elektronika **49** (9) 857–862 (2019)
Translated by V.L. Derbov

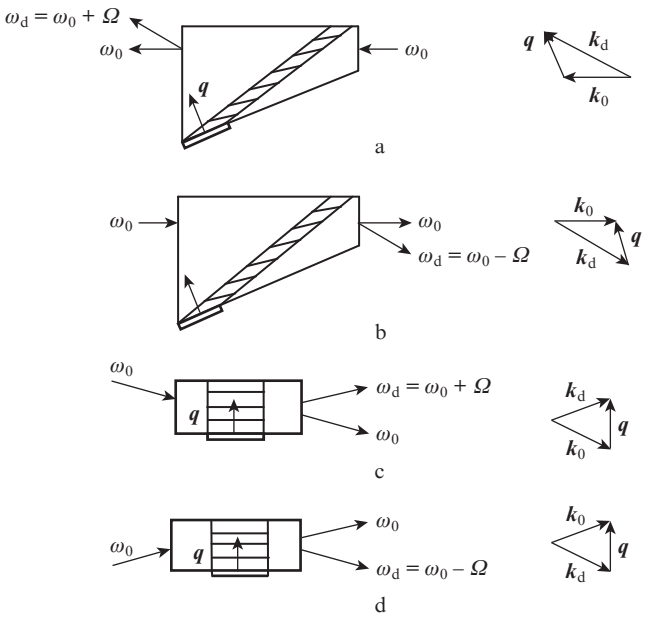

Figure 1. Schemes for using AO frequency shifters in the Bragg diffraction regime with (a, b) anisotropic and (c, d) isotropic diffraction to obtain (a, c) a positive and (b, d) negative frequency shift. The acoustic beam is indicated by hatching.

equal, $\Delta\omega = \Delta\Omega$, then their contributions to the frequency uncertainty of the diffracted wave are equal, too. The values of relative uncertainties differ by six orders of magnitude:

$$\frac{\Delta\Omega}{\Omega}\left(\frac{\Delta\omega}{\omega}\right)^{-1} = \frac{\omega}{\Omega} \approx 10^{14}\ \text{Hz}/10^{8}\ \text{Hz} = 10^{6}.$$

This fact should be taken into account when determining the requirements for the temporary stability of an ultrasound source under specific conditions.

It is necessary to define the terms. Since the frequency shift of the diffracted light wave is a direct consequence of AO diffraction, any AO cell can serve as a frequency shifter. The simplest AO device is an amplitude AO modulator (AOM), and therefore it is most often used as a frequency shifter. The requirements for the AOM usually contain speed restrictions, while the frequency shifters have no such requirements and operate in a continuous-wave regime. In this case, it is possible to use a slow transverse USW instead of a fast longitudinal one, which can dramatically increase the efficiency of AO diffraction and reduce the energy consumption of the device, increasing its reliability. In the future, in accordance with the established tradition for AO frequency shifters, we will use the term AOM, assuming that there are no requirements for the switching time.

The aim of this work is to develop AOMs optimised for use in optical and microwave QFS's based on cold strontium [3], rubidium [4], and caesium atoms with a spectral range of 460–900 nm and a frequency shift range of ±(5–400) MHz.

A peculiarity of using AOMs in QFS's is long (day or more) intervals of operation in the regime of continuous generation of light and ultrasound waves, as well as low power (tens of milliwatts) and small size (1–2 mm) of light beams. Therefore, the requirements for minimum power consumption were imposed on AOM in order to increase reliability, as well as reduce the size of light and sound waveguides, affecting the dimensions and cost of the device.

2. Calculation of the main AOM parameters

2.1. AO cell material

For the practical implementation of an AOM in the wavelength range 460–900 nm, a uniaxial birefringent positive tellurium dioxide crystal TeO_2 (paratellurite) was used, which has a unique combination of acoustic, optical, and AO properties [11], most important of which are large values of the quality parameter M_2 [5]. In TeO_2, effective diffraction of both isotropic and anisotropic types is possible. The radiation wavelength in vacuum λ and the ultrasonic frequency f are related as follows: for anisotropic diffraction in TeO_2 with the gyrotropy taken into account [12]

$$f = \frac{Vn_o}{\lambda} A(\gamma) A_1(\theta) [-B + (B^2 + C)^{1/2}], \tag{1}$$

where

$$A(\gamma) = (\mu^2 \cos^2\gamma + \sin^2\gamma)^{-1/2};$$

$$A_1(\theta) = (1 - \varkappa)[\cos^2\theta + (1 - \varkappa)^2 \sin^2\theta]^{1/2};$$

$$B = A(\gamma)(\mu'^2 \cos\gamma \sin\theta - \sin\gamma \cos\theta);$$

$$C = [(1 - \varkappa^2)^2 - 1]\cos^2\theta + (1 + \varkappa^2)[(1 - \varkappa)^4 - \mu^2]\sin^2\theta;$$

$$\mu = n_o/n_e; \quad \mu' = \mu(1 + \varkappa); \quad \varkappa = \rho\lambda/(2\pi n_o);$$

for isotropic diffraction in TeO_2 [5, 6] with $\boldsymbol{q} \| z$

$$f = \frac{2n_{o,e} V \tan\theta_B^{o,e}}{\lambda} \approx \frac{2\theta_B^{o,e} n_{o,e} V}{\lambda}, \tag{2}$$

where V is the USW velocity; n_o and n_e are the refractive indices of the ordinary and extraordinary beams in the crystal; γ is the angle between the wave vector $\boldsymbol{q}$ of the USW and the axis [110] of the crystal; θ is the angle between the wave vector of the incident ordinary light wave $\boldsymbol{k}_0^o$ and the z axis in the crystal; ρ is the specific rotatory power of TeO_2 in radians per unit length; and $\theta_B^{o(e)}$ is the angle between the wave vector of the ordinary (extraordinary) light wave in the crystal and the wave front of the USW.

It follows from Eqns (1) and (2) that for a fixed wavelength of light λ, by changing the angles of propagation of light and sound beams in the crystal θ, $\theta_B^{o,e}$ and γ, it is possible to obtain a frequency shift of the diffracted light wave without breaking phase matching in a wide range limited only by the operating band of the USW source, the width of which can reach an octave. In addition, the frequency shift is possible without mechanical adjustment of the crystal tilt angle within the width of the frequency instrument function of the AOM.

The AOM optimisation includes choosing the type of AO diffraction (isotropic, anisotropic), the regime of AO diffraction (Bragg, Raman–Nath) and the geometry of AO interaction (orientations of the wave vectors $\boldsymbol{k}_0$ and q relative to the crystallographic axes of TeO_2).

2.2. Selection of diffraction type

The wave vector diagrams for anisotropic and isotropic diffraction in TeO_2 are shown in Fig. 2. The subscripts of the

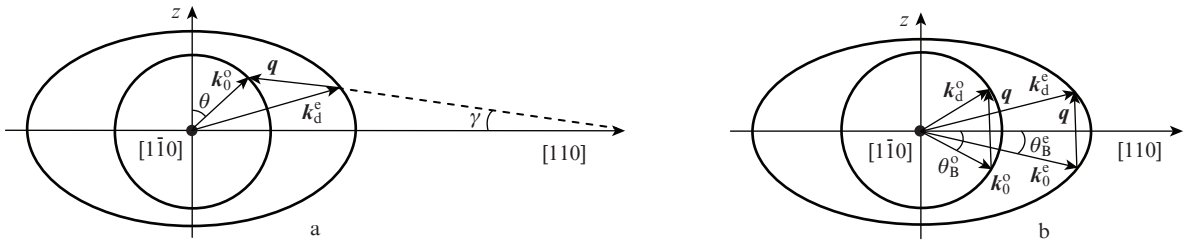

Figure 2. Diagram of wave vectors for (a) anisotropic and (b) isotropic diffraction in TeO_2.

wave vectors $\boldsymbol{k}_0^{o,e}$, $\boldsymbol{k}_d^{o,e}$ correspond to beams of incident and diffracted light waves, and the superscripts correspond to beams with ordinary (o) and extraordinary (e) polarisations in the crystal.

The AOM based on the geometry of Fig. 2b ($\boldsymbol{q}||z$) can operate efficiently regardless of the state of polarisation of the incident light beam. This feature is a consequence of two reasons. First, if the input and output optical faces of the AOM are parallel to the vector $\boldsymbol{q}$, an arbitrarily polarised light beam incident from air on the input face of the AOM at an angle

$$\alpha = n_o q/(2k_0^o) \approx \theta_B^o n_o \approx \theta_B^e n_e, \qquad (3)$$

propagates in the crystal at Bragg angles simultaneously for both mutually orthogonal polarisations. Similarly, diffracted beams will propagate in air in one direction in the form of a single light beam. Second, the effective photoelastic constants p_{13} and p_{33}, corresponding to the processes o → o and e → e, are respectively 0.34 and 0.24 [13]. In the approximation of plane light waves, it is easy to show [5] that in the nonlinear regime of diffraction by a single ultrasonic wave, the efficiency values for these processes can be equal and, in this case, are close to unity. We note that this is the only geometry known to us for TeO_2 that possesses such a practically important property.

The type of diffraction determines the functionality and features of AOMs. The main ones for AOMs based on isotropic and anisotropic diffraction in TeO_2 are listed below.

	AOMs based on isotropic difraction	AOMs based on anisotropic difraction
Polarisation of the incident and diffracted beams	parallel	orthogonal
Possibility of efficient operation with arbitrarily polarised radiation	present	absent
Ability to work using to the two-pass scheme of Fig. 3	present	absent
Possibility of increasing contrast when using polarisers	absent	present
Possible diffraction regimes	Bragg, Raman–Nath	Bragg
USW type	longitudinal	shear
USW velocity V/m s^{-1}	4200	620–900
Length-to-width ratio of the piezoelectric transducer L/H (Bragg regime)	10–20	3–7
High-frequency signal power required to a achieve maximum diffraction efficiency/W (Bragg regime)	~1	~(10^{-1}–10^{-2})

Figure 3 shows a two-pass optical scheme of the AOM. It allows doubling the frequency shift when using one AOM based on isotropic diffraction.

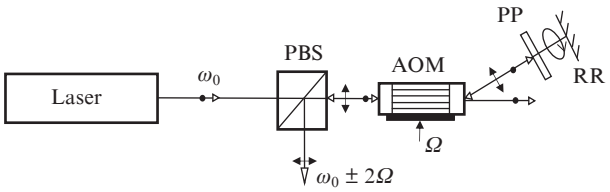

Figure 3. Double-pass optical scheme of the AOM to obtain a doubled frequency shift:
(PBS) polarisation beam splitter; (PP) quarter-wave phase plate; (RR) retroreflector.

The data listed above show that in the continuous-wave regime, anisotropic diffraction-based AOMs have advantages in size and power consumption, but they cannot be used in a two-pass scheme with the frequency shift doubling. In devices based on isotropic diffraction, the two-pass scheme is implemented, but this requires a significantly higher power of the control signal

2.3. Diffraction regime selection

For AOMs operating in laser cooling systems, it is preferable to use the purely Bragg diffraction regime, since it is necessary to ensure a frequency shift with minimal loss in the intensity of the laser beam [2–4]. On the contrary, for AOMs operating in systems of laser frequency stabilisation, the complete antisymmetry of diffraction reflections is important (the equality of amplitudes and diffraction angles of light waves corresponding to the diffraction orders ±1, their phase difference being equal to π). Therefore, the pure Raman–Nath regime is needed [7–10].

According to Ref. [14], the diffraction regime depends on the dimensionless Klein–Cook parameter $Q = 2\pi l\lambda/\Lambda^2$, where l is the AO interaction length and Λ is the ultrasound wavelength. In practice, Raman–Nath diffraction is observed at $Q \leqslant 0.3$, and Bragg diffraction at $Q \geqslant 4\pi$ [15].

2.4. Choice of the operating point on the frequency-angle dependence for the AOM

The operating frequency band of the AOM (the absolute value of the frequency shift) can be represented as a sum of the constant and variable components: $f \pm \delta f/2$.

In the case of isotropic diffraction (Fig. 2b), the constant part of f is provided for a single value of the incidence angle of the light beam on the input face α according to Eqn (3). The variable part of δf is provided by changing the beam angle in the working range of angles from $\alpha + \Delta\alpha$ to $\alpha - \Delta\alpha$, where δf and $\Delta\alpha$ are related by the formula $\delta f/2 \approx 2\Delta\alpha V/\lambda$, valid in the approximation of small values of $\Delta\alpha$, which do not exceed a few degrees for the range in question.

In the case of anisotropic diffraction (Fig. 2a), the region of operating points (pairs of angles γ and θ) is determined as a solution of the system of Eqn (1) and

$$\begin{aligned} f \pm \delta f/2 &= \frac{Vn_o}{\lambda} A(\gamma)A_1(\theta_1)\{-B(\theta_1) + [B^2(\theta_1) + C(\theta_1)]^{1/2}\}, \\ \theta_1 &= \theta + \arcsin(n_o \sin\Delta\alpha_1), \\ f \mp \delta f/2 &= \frac{Vn_o}{\lambda} A(\gamma)A_1(\theta_2)\{-B(\theta_2) + [B^2(\theta_2) + C(\theta_2)]^{1/2}\}, \\ \theta_2 &= \theta - \arcsin(n_o \sin\Delta\alpha_2) \end{aligned} \tag{4}$$

provided that the following inequalities are valid:

$$\Delta\alpha_{\min} \leqslant (\Delta\alpha_1, \Delta\alpha_2) \leqslant \Delta\alpha_{\max}, \tag{5}$$

$$|\Delta\alpha_1 - \Delta\alpha_2| \leqslant \delta. \tag{6}$$

Here, the angle θ corresponds to the normal incidence of the light beam on the input face of the AOM ($\alpha = 0$). The upper sign in Eqns (4) corresponds to the increasing function $f(\theta)$, and the lower sing to the decreasing one. Since the function $f(\theta)$ is nonlinear, the working angle interval is asymmetric in the general case, and $\Delta\alpha_1 \neq \Delta\alpha_2$. Restrictions on the values of $\Delta\alpha_1$, $\Delta\alpha_2$ and the asymmetry of the angular aperture δ are introduced based on the convenience of AOM practical application. From the obtained set of operating points, it is reasonable to use the point corresponding to the maximum value of the effective photoelastic constant p_{eff}. The angular dependence $p_{\text{eff}}(\theta,\gamma)$ for the considered case is given in Ref. [16].

The dependence $f(\theta)$ for a fixed value of γ can have extrema [17]. In this case, the operating point is selected in the descending or ascending section of the curve so that the frequency range of the AOM does not include extremum points. As an example, Fig. 4 shows the dependence of the USW frequency f on the angle of incidence of the light beam on the input face in the interval $-\Delta\alpha_2 < \Delta\alpha < \Delta\alpha_1$ under the matching conditions for the Foton-5203 AOM at $\gamma = 1.3°$ and $\lambda = 461$ nm. The dependence has a monotonically increasing segment between the minimum and maximum points near the point $\Delta\alpha = 0$. It corresponds to the angles $\gamma = 1.3°$ and $\theta = 18.52°$. In this case, $\partial f/\partial\theta$ varies slightly in the frequency range $f \pm \delta f/2 = 80 \pm 10$ MHz, and the working range of angles is quite symmetrical: $\Delta\alpha_1 = 6.69°$, $\Delta\alpha_2 = -6.71°$.

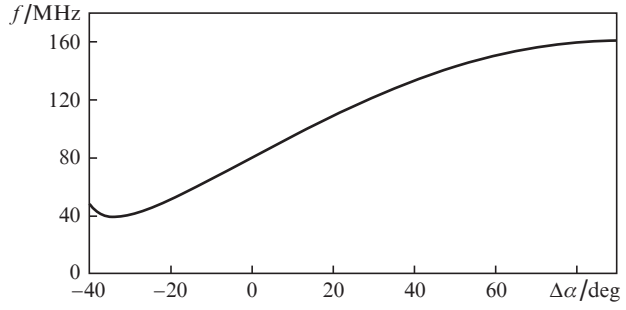

Figure 4. Dependence of the USW frequency f on the incidence angle $\Delta\alpha$ of a light beam with $\lambda = 461$ nm at the input face of the Foton-5205 AOM for $\gamma = 1.3°$.

2.5. Specific features of the AOM in the case of a diverging light beam

Relations (1) and (2) are valid for plane acoustic and light waves. In this case, the maximum value of the diffraction efficiency $\eta_m = I_d/I_0$, where I_d and I_0 are the intensities of the diffracted and incident light waves, respectively, is equal to 1. For a diverging beam, the value of η_m is smaller [18].

According to Ref. [19], for isotropic diffraction the quantity η_m depends on the parameter $a = d\theta/d\varphi$, where $d\theta \approx 1.27\lambda/(nD)$ is the total diffraction divergence of a light beam with Gaussian intensity distribution at the level $1/e^2$ in the medium; D is the initial diameter of the light beam; and $d\varphi = \Lambda/L$ is the divergence of the USW emitted by a homogeneous piezoelectric transducer of length L at an intensity level of 4 dB. For $a \ll 1$, the situation practically does not differ from the case of plane-wave diffraction, and $\eta_m \approx 1$. For $a = 1$ we have $\eta_m \approx 0.8$, and for $a = 2.8$ we obtain $\eta_m \approx 0.4$.

For anisotropic diffraction, a similar parameter $a' = \Delta f_{d\theta}/\Delta f$ can be introduced, where $\Delta f_{d\theta} \approx (df/d\theta)\Delta\theta(\Delta\alpha)$ is the frequency mismatch due to a change in the angle of incidence of the plane wave on the input face of the AOM (Fig. 3); and $\Delta f = V/[l\sin(\theta-\gamma)]$ is the width of the frequency instrument function of the AOM [16]. Similarly to the previous case, for $a' \ll 1$ we obtain $\eta_m \approx 1$.

Based on the above relations, the maximum length of the piezoelectric transducer was determined, at which the specified value η_m can be achieved.

3. Results of AOM experimental study and their discussion

A series of AOMs was developed, manufactured and investigated for use in optical and microwave frequency standards based on cold atoms of strontium [3], rubidium [4] and caesium. The main technical parameters were experimentally determined, namely, the working frequency band $f \pm \delta f/2$, the maximum value of the diffraction efficiency η and the power of the high-frequency signal necessary to achieve it. The data obtained are presented in Tables 1 and 2, which also show the values of the active AOM aperture equal to the width H of the piezoelectric transducer.

When working with high-frequency Foton 3204, 3205 AOMs, it is necessary to use a lens to focus the light beam into the sound column of size $L \times H$ (along and across the direction of light propagation). To estimate the focal length F of the lens and the size σ of the light beam waist in the focal plane, we take $a = 1$ ($\eta_m \approx 0.8$). Then $d\theta \approx D/(Fn) = d\varphi = V/(Lf)$ and for $D = 1$ mm, $n = 2.2$, $V = 4200$ m s^{-1}, $f = 400$ MHz, and $L = 2.5$ mm, we obtain $F \approx 110$ mm and $\sigma = 1.27\lambda F/D \approx 0.1$ mm $< H = 0.2$ mm. The actual value of F was determined empirically and amounted to 100–130 mm. When replacing a spherical lens with a cylindrical one to focus the beam in the plane orthogonal to the diffraction plane, the efficiency in the linear diffraction regime increases by ~30%, ceteris paribus. A useful result of spherical focusing is also the reduction of the device rise

Table 1. Technical parameters of AOMs operating in the Bragg diffraction regime for optical QFS's based on cold strontium atoms.

AOM name	Diffraction type	Radiation wavelength/nm	Operating frequency band/MHz	Light beam polarisation	First-order diffraction efficiency (%)	Active aperture/mm	High-frequency control signal power/W
Foton-5201	anisotropic	690 ± 40	40 ± 5	linear	⩾ 90	3.5	0.15
Foton-5202	anisotropic	500 ± 30	80 ± 10	linear	⩾ 90	3.5	0.06
Foton-5205	anisotropic	460 ± 30	80 ± 10	linear	⩾ 90	3.5	0.05
Foton-5211	anisotropic	680 ± 40	80 ± 10	linear	⩾ 90	3.5	0.15
Foton-5212	anisotropic	710 ± 40	80 ± 10	linear	⩾ 90	3.5	0.15
Foton-5206	anisotropic	460 ± 30	90 ± 10	linear	⩾ 90	3.5	0.04
Foton-5207	anisotropic	460 ± 30	110 ± 10	linear	⩾ 90	3.5	0.04
Foton-5203	anisotropic	690 ± 40	110 ± 10	linear	⩾ 90	3.5	0.15
Foton-5204	anisotropic	690 ± 40	150 ± 10	linear	⩾ 90	3	0.4
Foton-3211	isotropic	690 ± 40	80 ± 10	arbitrary	⩾ 90	1.6	0.7
Foton-3212	isotropic	690 ± 40	110 ± 10	arbitrary	⩾ 90	1.2	0.6
Foton-3208	isotropic	690 ± 40	400 ± 100	arbitrary	⩾ 60	0.2	1.0

Table 2. Technical parameters of AOMs for microwave QFS's on cold rubidium and caesium atoms.

AOM name	Diffraction type and regime	Radiation wavelength/nm	Operating frequency band/MHz	Light beam polarisation	First-order diffraction efficiency (%)	Active aperture/mm	High-frequency control signal power/W
Foton-3201	isotropic, Bragg	780 ± 40	80 ± 20	arbitrary	⩾ 90	2	1.5
Foton-5208	anisotropic, Bragg	780 ± 40	170 ± 10	linear	⩾ 70	2.8	0.3
Foton-5209	anisotropic, Bragg	780 ± 40	230 ± 10	linear	⩾ 70	2.3	0.5
Foton-3207	isotropic, Raman–Nath	780 ± 40	5–10	arbitrary	∼ 10*	2	0.1
Foton-3204	isotropic, Raman–Nath	850 ± 40	20–40	arbitrary	∼ 10*	2	0.4
Foton-3205	isotropic, Raman–Nath	780 ± 40	20–40	arbitrary	∼ 10*	2	0.5

* Diffraction efficiency in the diffraction orders ±1.

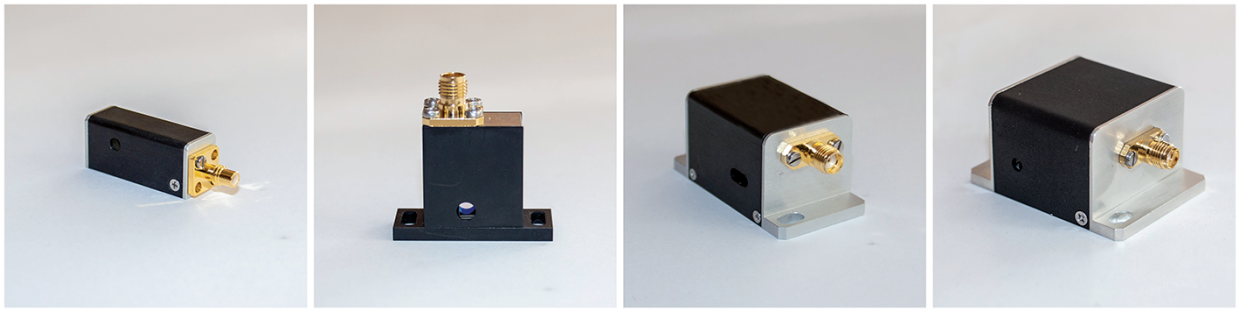

a b c d

Figure 5. (a) Foton-3204, 3205; (b) Foton-3208; (c) Foton-5201–5209, 5211, 5212; and (d) Foton-3201, 3207, 3211, 3212 AO modulators/frequency shifters for frequency standards using cold strontium, rubidium and caesium atoms.

time τ_r [19]: $\tau_r \approx 0.64H/V \approx 30$ ns. Therefore, this device can be used as a key modulator of the laser cavity Q factor.

Figure 5 shows photographs of four types of AOMs [20]. The range of overall dimensions was 12–50 mm; the mass range was 20–60 g. High-frequency connectors of SMA and SMC types were used.

4. Conclusions

The possibilities of optimising frequency-shifting AO modulators for use in laser cooling systems and stabilisation of laser sources are considered.

A series of specialised AOMs is developed for optical and microwave frequency standards based on cold atoms of strontium, rubidium, and caesium, and their parameters are experimentally studied.

The modulators operate with linearly and arbitrarily polarised radiation and have a high diffraction efficiency, small size and mass and low power consumption.

It should be noted that the scope of the AOMs developed and presented here is much wider than the QFS's based on slow atoms. Foton-3207 and Foton-5208 models can also find application in the development of advanced small-size microwave QFS's based on a rubidium gas cell with pulsed optical pumping [21].

References

1. Riehle F. *Frequency Standards: Basics and Applications* (Weinheim: Wiley, 2006; Moscow: Fizmatlit, 2009).
2. Khabarova K.Yu., Slyusarev S.N., Strelkin S.A., Belotelov G.S., Kostin A.S., Pal'chikov V.G., Kolachevsky N.N. *Quantum Electron.*, **42**, 1021 (2012) [*Kvantovaya Elektron.*, **42**, 1021 (2012)].

3. Berdasov O.I., Gribov A.Yu., Strelkin S.A., Slyusarev S.N. *Al'manakh Sovremennoi Metrologii*, **11**, 81 (2017).
4. Kupalov D.S., Baryshev V.N., Blinov I.Yu., Boiko A.I., Domnin Yu.S., Kopylov L.N., Kupalova L.N., Novoselov A.V., Khromov M.N. *Al'manakh Sovremennoi Metrologii*, **11**, 95 (2017).
5. Magdich L.N., Molchanov V.Ya. *Acousto-optic Devices and Their Applications* (New York: Gordon and Breach Science Publishers, 1989; Moscow: Sov. radio, 1978).
6. Balakshiy V.I., Parygin V.N., Chirkov L.E. *Fizicheskiye osnovy acustooptiki* (Physical Foundations of Acousto-optics) (Moscow: Radio i svyaz', 1985) p. 280.
7. Baryshev V.N., Epikhin V.M. RF Patent No. 2445663. Priority date 19 October 2012.
8. Baryshev V.N., Epikhin V.M. *Quantum Electron.*, **40**, 431 (2010) [*Kvantovaya Elektron.*, **40**, 431 (2010)].
9. Baryshev V.N. *Quantum Electron.*, **42**, 315 (2012) [*Kvantovaya Elektron.*, **42**, 315 (2012)].
10. Baryshev V., Epikhin V., Blinov I., Donchenko S. *Proc. 2016 IEEE Int. Frequency Control Symp*. (New Orleans, Louisiana, USA, 2016) p. 205.
11. Blistavan A.A., Bondarenko V.S., Perelomova N.S., Strizhevskaya F.N., Chkalova V.V., Shaskol'skaya M.P. *Akusticheskiye kristally* (Acoustic Crystals) (Moscow: Nauka, 1982) p. 632.
12. Epikhin V.M. *Tech. Phys.*, **40**, 903 (1995) [*Zh. Tekh. Fiz.*, **65** (9), 71 (1995)].
13. Uchida N., Ohmachi Y. *J. Appl. Phys.*, **40** (12), 4692 (1969).
14. Klein W.R., Cook B.D. *IEEE Trans.*, **SU-14**, №3, 123 (1967).
15. Uchida N., Niizeki N. *Proc. IEEE*, **61** (8), 1073 (1973).
16. Epikhin V.M., Vizen F.L., Pal'tsev L.L. *Zh. Tekh. Fiz.*, **57** (10), 1910 (1987).
17. Epikhin V.M., Vizen F.L., Nikitin N.V., Kalinnikov Yu.K. *Sov. Phys. Tech. Phys.*, **27**, 1482 (1982) [*Zh. Tekh. Fiz.*, **52** (12), 2405 (1982)].
18. Magdich L.N., Molchanov V.Ya. *Opt. Spektrosk.*, **48** (1), 159 (1980).
19. Maydan D. *IEEE J.*, **QE-6**, №1, 15 (1970).
20. www.aodevices.ru.
21. Baryshev V.N., Aleinikov M.S., Osipenko G.V., Blinov I.Yu. *Quantum Electron.*, **48**, 443 (2018) [*Kvantovaya Elektron.*, **48**, 443 (2018)].